Chapter 9

Imaging of Rheumatoid Arthritis

RA is one of the most common diseases of human joints of the hands and feet. It affects 1-2% of the world population and 2.1 million people in the United States [Lawrence98]. It is a progressive disease characterized by an inflammation process, which currently can not be cured. Furthermore, routine imaging techniques for early diagnosis do not exist. Applying optical image reconstruction methods to this problem is difficult, because of a clear fluid present within the joint. MOBIIR schemes based on the diffusion equation do not allow an accurate calculation of the fluence in these low scattering areas [Firbank96] [Hielscher98] [Dehghani99] [Riley00].

We developed a transport-theory-based MOBIIR scheme for reconstructing optical parameters. So far, this technique was experimentally evaluated on tissue phantoms that contained void-like regions. As first biomedical application we focused on early diagnosis and monitoring of RA in *proximal interphalangeal* (PIP) joints. First, we carried out a quantitative study for monitoring RA based on a numerical PIP joint model. Second, we show the first sagittal image of optical parameters in a human PIP joint.

9.1 Rheumatoid Arthritis

RA is a progressive disease and is characterized by an inflammation process that originates in the inner membrane (*synovial membrane* or *synovium*) of the joint capsule and spreads to other parts of the joint. The rheumatoid inflammation process can generally be divided into different stages. During the first stage of the inflammation process the synovium starts to swell and changes its permeability. Dissolved and detached cells of the capsule migrate into the *synovial cavity* that is occupied by the *synovial fluid*. This also leads to changes in the optical parameters of the synovium and the synovial fluid [Beuthan96b] [Prapavat97]. During the second stage parts of the capsule are growing into the synovial cavity. The cavity becomes physically smaller, and the synovial fluid becomes more turbid. In the later stages, the rheumatoid inflammation process destroys the capsule entirely and starts to attack the bone.

Diagnosing RA can be difficult because some symptoms are common to many different diseases. A physician will review the patient's medical history, obtain laboratory test, and may order imaging procedures to make a diagnosis. Imaging techniques like x-ray shadowgrams or CAT (see Chapter 1.1) are only able to monitor hard tissues with a high sensitivity, but they do not show soft tissues such as the cartilage, the inner membrane, or the synovial fluid. They are not able to monitor the early inflammation process characterized by slight changes of the properties of the synovial fluid and the synovium. Therefore, x-ray techniques are used for advanced rheumatoid stages with partly damaged bones in the region of the cavity [Sharp95]. Ultra sonic imaging techniques only allow to recover boundary layers, where the refractive index of ultra sonic waves is changed. It is mainly used in large joints, such as the shoulder. Ultrasound fails to detect very early stages of the inflammation, when significant changes of the thickness of the capsule have not yet been

occurred [Lehtinnen96]. MRI (see Chapter 1.1) can be used to recover changes of soft tissues when contrast agents are used. These agents provide greater contrast between normal and abnormal tissue in the body. The contrast agent Gadolinium, a non-radioactive clear fluid, is intravenously injected. It accumulates in blood vessels and has the effect of making vessels and highly vascular tissues appear brighter. Inflamed tissue, such as the capsule of a PIP joint affected by RA, becomes very bright (enhanced) on the MRI (see Figure 9.1) [Ostergaard97]. Gadolinium is then rapidly cleared from the body by the kidneys. However, MRI is currently still too expensive for long-term, routine monitoring of RA.

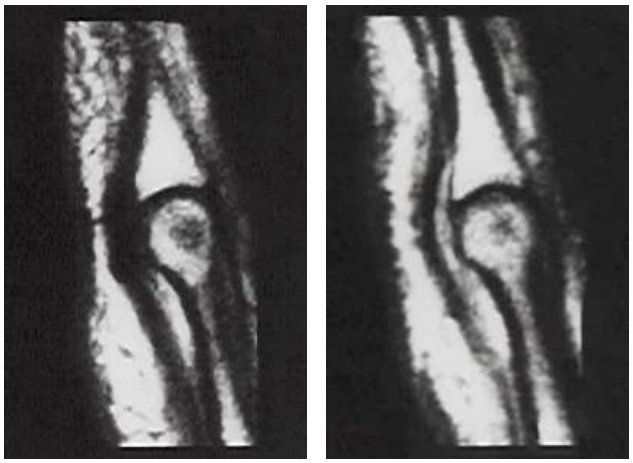

(a) Healthy condition.

(b) Rheumatoid condition with severe inflammation.

Figure 9.1: Sagittal MRIs of human PIP joints with the interior surface on the left. Images were taken from a 60 years old male patient with RA. The image of the healthy condition of the PIP joint was taken without a contrast agent. The image of the rheumatoid condition of the PIP joint was taken on the other hand with the contrast agent Gadolinium. The inflamed joint capsule appears very bright in the image.

9.2 Optical Monitoring of Rheumatoid Arthritis

Given the process of the inflammatory disease RA, information about the optical properties of the synovium, obtained from OT, could be used to distinguish between healthy and early rheumatoid conditions. Additionally, the optical properties of the synovial fluid indicate the various stages of the inflammation process. Therefore, optical techniques could not only be used to detect early stages of RA but also monitor the inflammation process during the administration of medication. The rheumatoid inflammation is not a steady state but rather an alternating process between highly inflamed and more or less relaxed conditions, which could be optically monitored.

9.2.1 Finger Joint Model

In our studies concerning RA, we focused on PIP joints. PIP joints are suitable for NIR transillumination [Beuthan96b], because of their small geometry. The major components of this finger joint system are the bones, cartilage, muscle, tendon, ligament, and the joint capsule. In the joint two bones are connected and are kept movable around one axis. The bones belong to hard tissue and are covered with a protective cartilage layer within the joint. The capsule is a soft tissue and connects the bones of the finger and confines the joint. The joint cavity between the two finger bones has a size of approximately 200 μm and is filled with the almost non-scattering synovial fluid, which keeps the joint movable and provides nutrition to the cartilage. The ligament and the tendon are also soft tissue and connect the two bones or the bone with the muscle, respectively.

We have developed a two-dimensional numerical model for the optical properties of a sagittal cross-section of a PIP joint, assuming a finger with a thickness of 2 cm. The optical parameters, μ_s and μ_a, were assigned to different tissue parts, such as bone, tendon, muscle, capsule, and synovial fluid. The reduced scattering coefficient, μ_s', and the absorption

coefficient, μ_a, of bone tissue, the capsule, and the synovial fluid of finger joints were given for $\lambda = 685$ nm by Prapavat *et al* [Prapavat97]. The optical parameters of the tendon and muscle were not experimentally known. Thus, we assumed values for these tissue types as given in Table 9.1. Furthermore, the anisotropy factor was taken to be constant $g = 0.9$ for all tissue types. The reduced scattering coefficient, μ_s', which was given experimentally, had to be transformed with $\mu_s' = (1 - g)\mu_s$ into the scattering coefficient, μ_s. The anisotropy factor $g = 0.9$ was assumed to be spatially constant. The optical parameters of all tissue types for the healthy condition and the early stages of RA are given in Table 9.1.

	healthy μ_s in cm^{-1}	rheumatoid μ_s in cm^{-1}	healthy μ_a in cm^{-1}	rheumatoid μ_a in cm^{-1}
bone	210	210	0.8	0.8
tendon	80	80	0.5	0.5
muscle	100	100	0.7	0.7
capsule	60	110	1.5	2.4
synovial fluid	0.6	1.2	0.04	0.11

Table 9.1: Optical parameters of the numerical PIP joint model. The anisotropy factor was assumed to be constant with $g = 0.9$.

The numerical joint model we used for this study had dimensions of 4 cm $\times$ 2 cm. A sagittal cross-section of the PIP joint was discretized on a 161×81 grid (see Figure 9.2). The step size between two grid points was $\Delta x = \Delta y = 0.025$ cm. It was necessary to choose such a small grid point separation because of the small cavity between the two bones. 10 different sources were placed on the interior surface of the finger model with a separation of 0.2 cm. On the opposite side of the finger we positioned 30 detectors with a separation of 0.1 cm. Synthetic measurement data were calculated by using 16 ordinates and the relatively fine finite-difference mesh.

We used the numerical joint model as described above and changed the optical

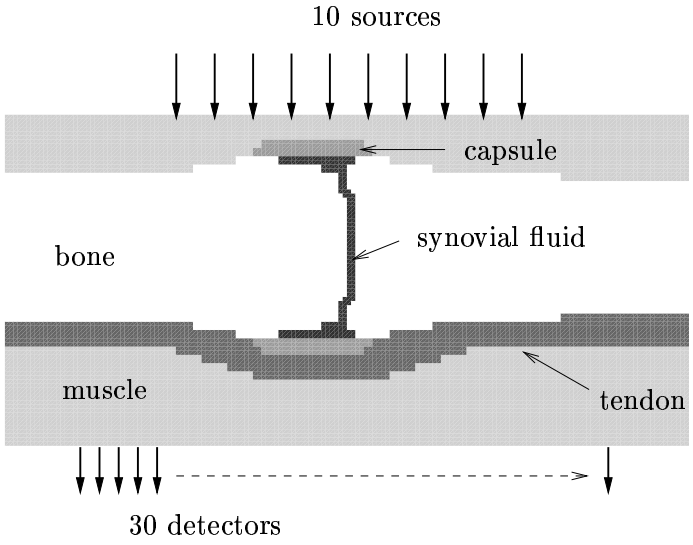

Figure 9.2: Numerical PIP joint model with sagittal cross-section. Sources were placed on the interior side of the finger.

parameters of different tissue parts according to the healthy and rheumatoid condition of the finger joint. First, we simulated the healthy condition of the joint and calculated the synthetic measurement data. Second, we changed the optical parameters either of the synovial fluid or of the capsule, depicting a rheumatoid condition. Last, we changed the optical parameters of both capsule and synovial fluid. We did not consider swelling of the joint due to the inflammation process, which typically occurs in later stages of RA, and therefore the geometry of all tissue types were kept constant. The fluence ϕ at the detector positions was normalized to its average value of all 10×30 measurement points (see also Equation 3.1).

9.2.2 Numerical Results

The synthetic measurement data of all four different conditions of the numerical PIP joint model became input to the MOBIIR scheme. The optical parameters, μ_s and μ_a,

were reconstructed on a 81×41 mesh with a grid point separation of $\Delta x = \Delta y = 0.05$ cm. Here, we have chosen a coarser finite-difference mesh than previously used for the calculation of the synthetic measurement data. That was necessary because of the computational burden of the adjoint differentiation technique, which had to store the radiance ψ_{kij} of all grid points and ordinates for each iteration step z of the SOR method. We employed the CG method for minimizing the objective function. The CG method took approximately 430-460 forward and 40-43 gradient calculations until the relative difference $|(\Phi_{k+1} - \Phi_k)/\Phi_k|$ of the objective function at two subsequent iteration steps was less than $\epsilon = 0.03$.

The reconstruction process was started with a homogeneous initial guess of $\mu_{s_0} = 100\ \text{cm}^{-1}$ and $\mu_{a_0} = 0.7\ \text{cm}^{-1}$. The reconstructed results of μ_s and μ_a for the healthy joint, the rheumatoid joint with altered synovial fluid, the rheumatoid joint with altered capsule, and finally, the rheumatoid joint where both tissue parts were changed simultaneously are shown in Figure 9.3 and Figure 9.4. The difference between adjacent isolines is $\mu_s = 10\ \text{cm}^{-1}$ and $\mu_a = 0.04\ \text{cm}^{-1}$.

The images in Figures 9.3 and 9.4 show clearly both bones enclosing the joint cavity in the center of the image. The left and right-hand side of the images show artifacts due to lack of source and detector positions. Therefore, these areas contain mostly the optical parameters of the unchanged initial guess. Artifacts do also occur in the vicinity of the source and detector positions with largely increased or decreased optical parameters.

The cavity between the two bones and the capsule on the interior side of the finger were smaller in the reconstructed images of the scattering coefficient than in the images of the absorption coefficient. This was already found in other reconstructions, such as the reconstruction of the void-like ring (see Figure 8.5 on page 137), where the ring was broadened in the μ_a-image. We also found that changes of the synovial fluid show up in images of μ_a, even when the synovial fluid was not altered in the numerical model (see

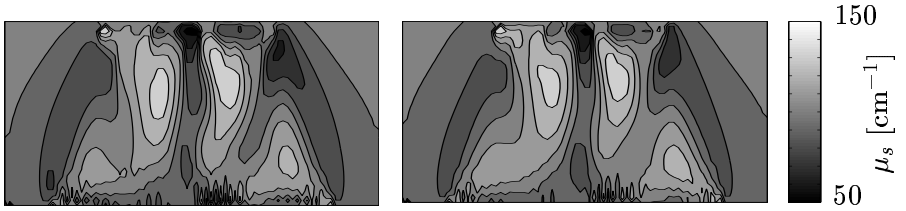

(a) Reconstructed healthy finger joint.

(b) Reconstructed rheumatoid finger joint with altered optical parameters of the synovial fluid.

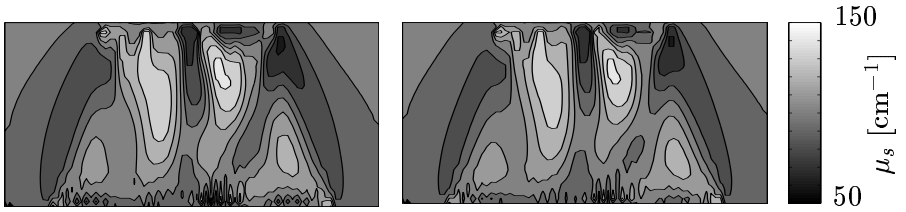

(c) Reconstructed rheumatoid finger joint with altered optical parameters of the capsule.

(d) Reconstructed rheumatoid finger joint with altered optical parameters of the capsule and synovial fluid.

Figure 9.3: Reconstructed scattering coefficient μ_s of the numerical PIP joint model of the healthy and early rheumatoid condition. The optical parameters of the rheumatoid condition were altered according to Table 9.1. The homogeneous initial guess of the reconstruction process was $\mu_{s_0} = 100$ cm^{-1} and $\mu_{a_0} = 0.7$ cm^{-1}. The distance between adjacent isolines is $\mu_s = 10$ cm^{-1}.

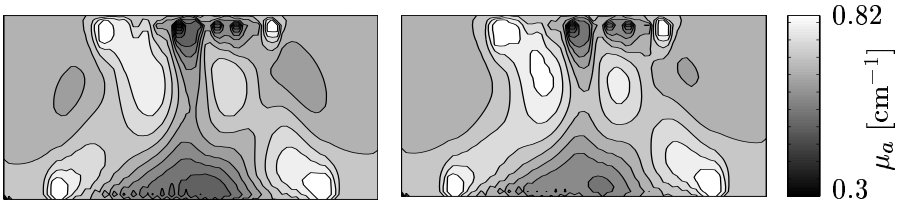

(a) Reconstructed healthy finger joint.

(b) Reconstructed rheumatoid finger joint with altered optical parameters of the synovial fluid.

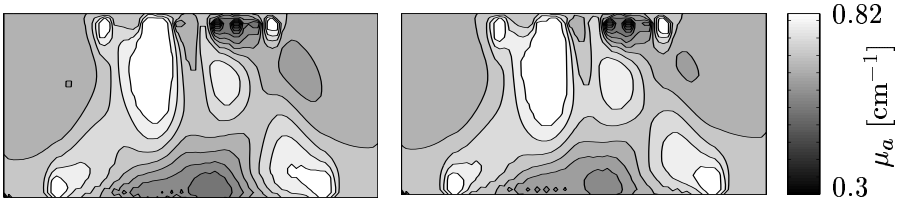

(c) Reconstructed rheumatoid finger joint with altered optical parameters of the capsule.

(d) Reconstructed rheumatoid finger joint with altered optical parameters of the capsule and synovial fluid.

Figure 9.4: Reconstructed absorption coefficient μ_a of the numerical PIP joint model of the healthy and rheumatoid condition. The optical parameters of the rheumatoid condition were altered according to Table 9.1. The homogeneous initial guess of the reconstruction process was $\mu_{s_0} = 100$ cm^{-1} and $\mu_{a_0} = 0.7$ cm^{-1}. The distance between adjacent isolines is $\mu_a = 0.04$ cm^{-1}.

Figure 9.4(c)). This phenomenon is partly due to changes of the optical parameters of the capsule, which obviously has an impact on the synovial fluid in the reconstructed image.

The main focus of this study was to differentiate between the healthy and the rheumatoid condition. A method for differentiating quantitatively images of healthy, μ^h, and rheumatoid, μ^{RA}, conditions is by taking the ratio

$$q = \frac{\mu^{RA} - \mu^h}{\mu^h} \tag{9.1}$$

of both images for either μ_s (see Figure 9.5) or μ_a (see Figure 9.6). First, maximum relative changes of 9% for μ_s and 7.4% for μ_a occur (see Figure 9.5(a) and Figure 9.6(a)) when only the optical parameters of the synovial fluid were altered. Second, altering the optical parameters of the capsule leads to maximum relative changes of 24% in the reconstructed image of μ_s and of 32% in the reconstructed image of μ_a (see Figure 9.5(b) and Figure 9.6(b)). The maximum changes of the reconstructed optical parameters occur at the position of the upper part of the capsule, which was closest to the interior surface of the joint. Last, the maximum relative change of μ_s is 28%, while μ_a changed by 34% (see Figure 9.5(c) and Figure 9.6(c)) when the optical parameters of the capsule and the synovial fluid were altered simultaneously. In conclusion, relative changes of the reconstructed optical parameters of the capsule appear to be more significant than relative changes of the optical parameters of the synovial fluid. Another observation is that reconstructed images of μ_a (Figure 9.4) have less artifacts than the reconstructed images of μ_s (Figure 9.3). The same holds for the ratio-images (see Figures 9.5 and 9.6).

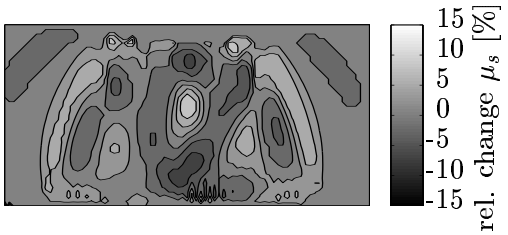

(a) Synovial fluid of joint model was changed (distance between isolines is 2.5%).

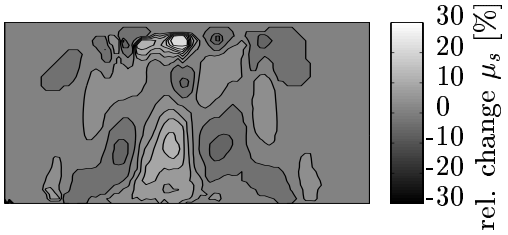

(b) Capsule of joint model was changed (distance between isolines is 3%).

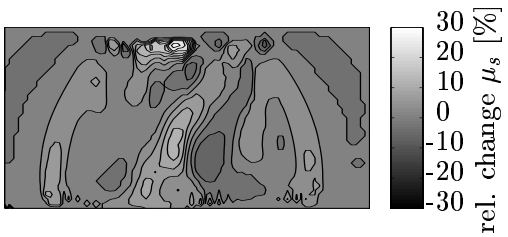

(c) Capsule and synovial fluid of joint model were changed (distance between isolines is 3%).

Figure 9.5: Relative change in μ_s of the reconstructed rheumatoid PIP joint with respect to the reconstructed healthy PIP joint.

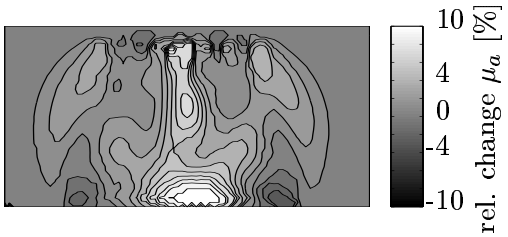

(a) Synovial fluid of joint model was changed (distance between isolines is 1%).

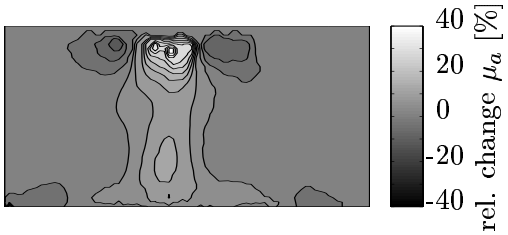

(b) Capsule of joint model was changed (distance between isolines is 4%).

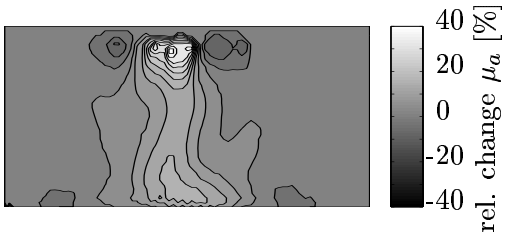

(c) Capsule and synovial fluid of joint model were changed (distance between isolines is 4%).

Figure 9.6: Relative change in μ_a of the reconstructed rheumatoid PIP joint with respect to the reconstructed healthy PIP joint.

9.3 Reconstruction of a Human Finger Joint

In the previous section we compared in a numerical study reconstructed images of the healthy and early rheumatoid conditions. We used the MOBIIR scheme to reconstruct sagittal cross-sections of the scattering and absorption coefficients in a numerical PIP joint model. Now, we applied the MOBIIR scheme to experimental data obtained from a real human finger joint.

We performed measurements on a PIP joint (middle finger, right hand) of a 25 years old male proband (Figure 9.7). The finger had an approximately conic shape with a plane posterior side and an oblique interior side. The experimental set-up was similar to that used in Section 4.1, however another light source and detection system were used.

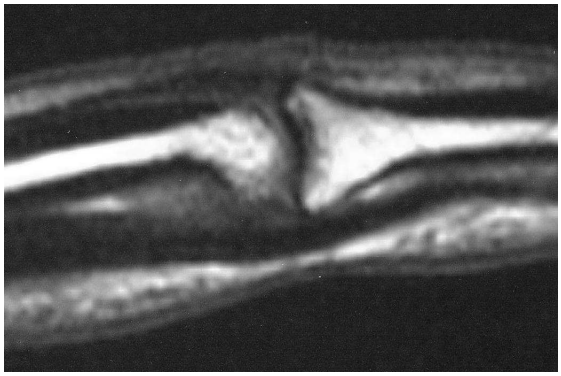

Figure 9.7: MRI of the human PIP joint with the interior side on the top. The synovial cavity between the two bones that is filled with synovial fluid is clearly visible in the center of the image.

A laser diode illuminated the interior side of the PIP joint at 11 different positions with a spatial separation of 0.2 cm. The laser spot on the finger surface had a diameter of 0.1 cm. We used a wavelength of $\lambda = 678$ nm. A silicon diode measured the transmitted

fluence on the posterior side of the joint at 16 different positions with a spatial separation of 0.2 cm. The aperture angle of the detector was 50^{o}. The distance of the detector to the surface of the finger was approximately 0.3 cm that resulted in a relatively large detection spot with a diameter of approximately 0.33 cm. The source-detector configuration yielded $D = 11 \times 16$ measurement points, which became subsequently input to the MOBIIR scheme. A schematic of the experimental set-up is shown in Figure 9.8.

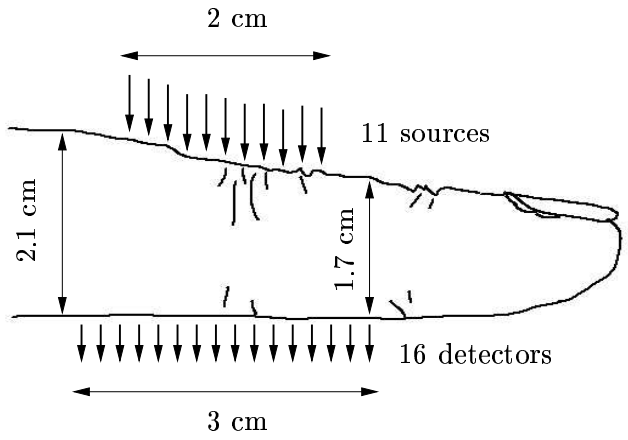

Figure 9.8: Schematic of human finger (PIP joint) with source-detector configuration. Sources were placed on the interior side and detectors were placed on the posterior side of the finger.

The optical parameters were reconstructed on a finite-difference grid to obtain sagittal images of μ_s and μ_a of the finger joint. The mesh covered a cross-sectional area of 4 cm $\times$ 2.1 cm of the finger. We used 81 $\times$ 43 grid points with a separation of $\Delta x = \Delta y = 0.05$ cm and 16 discrete ordinates. The detectors were placed on the bottom of the mesh along the boundary. However, the sources were partly positioned within the grid on interior grid points because of the oblique upper surface of the finger. Each forward calculation within the MOBIIR scheme used a constant anisotropy factor of $g = 0.9$

and Fresnel boundary conditions with a refractive index of $n = 1.5$. The overrelaxation parameter of the SOR method was $\rho = 1.5$.

We employed the CG method within the MOBIIR scheme to reconstruct μ_s and μ_a. The reconstruction started from an initial guess $\mu_{s_0} = 100$ cm^{-1} and $\mu_{a_0} = 0.7$ cm^{-1}. It was the same initial guess as used for the numerical study in Subsection 9.2.2. The optimization process was terminated after the condition $|(\Phi_{k+1} - \Phi_k)/\Phi_k| < \epsilon = 10^{-4}$ was satisfied. 140 forward and gradient (133+7) calculations were necessary for the image reconstruction.

The reconstructed images of μ_s and μ_a are shown in Figure 9.9 and Figure 9.10. The top of the images depicts the interior side and the bottom of the images constitutes the posterior side of the finger. The right-hand side of the images points towards the finger tip. Figure 9.9 shows the scattering coefficient on a scale from $\mu_s = 40$ cm^{-1} to $\mu_s = 160$ cm^{-1}. The difference between two neighboring isolines is $\mu_s = 10$ cm^{-1}. The absorption coefficient is shown in Figure 9.10 on a scale from $\mu_a = 0.5$ cm^{-1} to $\mu_s = 1.1$ cm^{-1}. Adjacent isolines are separated by $\mu_a = 0.05$ cm^{-1}.

The reconstructed scattering and absorption coefficients show clearly the synovial fluid in the center of the images. The smallest values are $\mu_s = 43$ cm^{-1} and $\mu_a = 0.52$ cm^{-1}. The reconstructed optical parameters are not as small as the real optical parameters of the synovial fluid within the joint cavity. Thus, the area of the cavity in the image, which is covered by the decrease of optical parameters, is larger than the real joint cavity. The adjacent tissue parts to the left and to the right in the image depict the bones. We find here an increase of both optical parameters with approximately $\mu_s = 150$ cm^{-1} and $\mu_a = 0.9$ cm^{-1}.

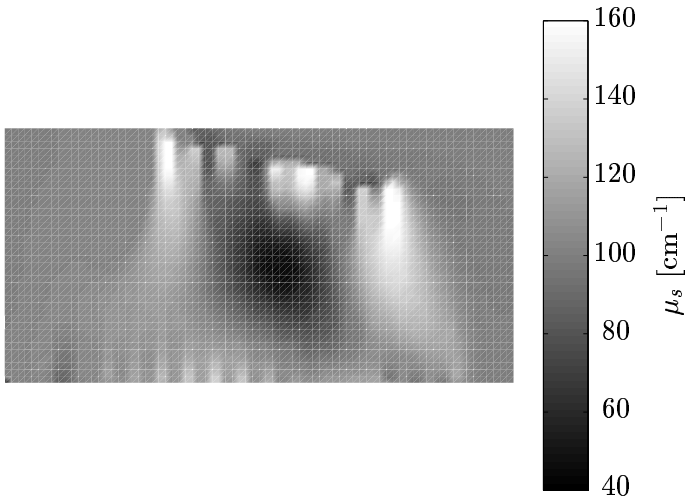

(a) Grayscale image of the PIP joint.

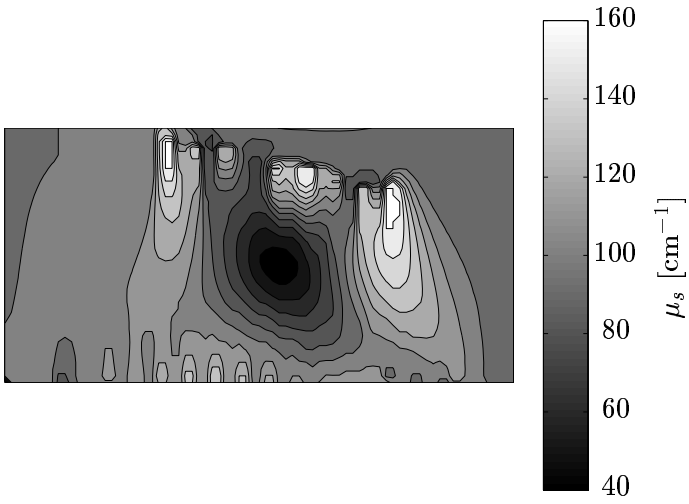

(b) Contourplot of the PIP joint. Adjacent isolines are separated by $\mu_s = 10$ cm^{-1}.

Figure 9.9: Sagittal image of the reconstructed scattering coefficient μ_s. The image has a length of 4 cm and a height of 2.1 cm. The interior side of the finger is on the top. The finger tip is towards right. Small μ_s of the synovial fluid are visible in the center of the image.

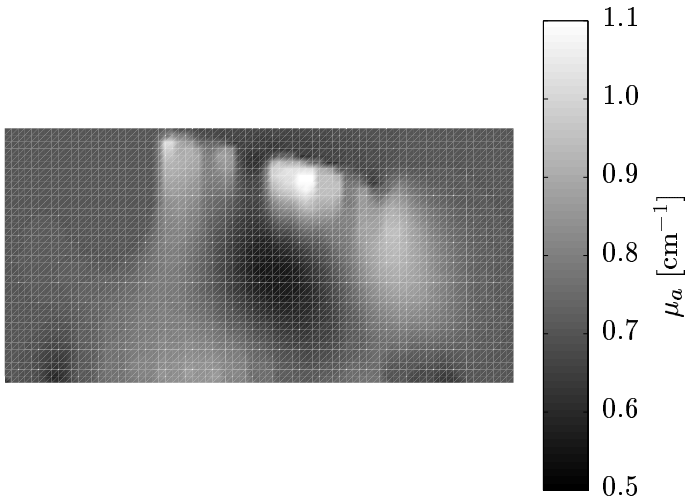

(a) Grayscale image of the PIP joint.

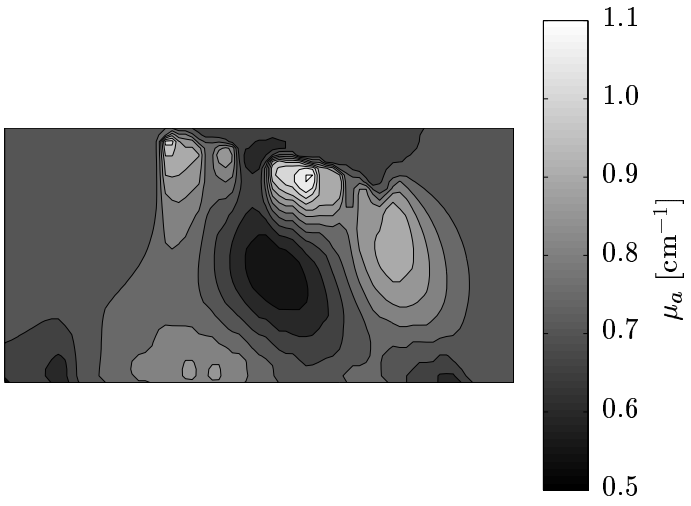

(b) Contourplot of the PIP joint. Adjacent isolines are separated by $\mu_a = 0.05$ cm^{-1}.

Figure 9.10: Sagittal image of the reconstructed absorption coefficient μ_a. The image has a length of 4 cm and a height of 2.1 cm. The interior side of the finger is on the top. The finger tip is towards right. Small μ_a of the synovial fluid are visible in the center of the image.

9.4 Discussion

We performed a numerical study to distinguish between the healthy and an early rheumatoid condition of a human PIP joint by using synthetically generated measurement data. Thus, we reconstructed sagittal cross-sectional images of μ_s and μ_a of a numerical PIP joint model. The results show that altered optical parameters of the joint model depicting the rheumatoid condition are difficult to recover if we only consider absolute values of reconstructed optical parameters (e.g. Figures 9.3(d) and 9.4(d)). However, if we consider the relative change of the reconstructed optical parameters of the rheumatoid with respect to the healthy joint then we can differentiate between both conditions (e.g. Figures 9.5(c) and 9.6(c)). This result implies that relative changes of the optical parameters of a PIP joint with different conditions might give more information about the joint condition than absolute values of the reconstructed optical parameters.

Furthermore, we reconstructed cross-sectional images of μ_s and μ_a of a human PIP joint (see Figures 9.9 and 9.10). The reconstructed images show clearly the synovial fluid in the center of the images. The reconstructed optical parameters of the synovial fluid within the joint cavity are decreased with respect to the initial guess by 67% for μ_s and by 26% for μ_a. The area in the image occupied by the synovial fluid is approximately 0.8 cm $\times$ 0.6 cm, and is larger than the area of the joint cavity in the finger. That can have several reasons. First, we applied a two-dimensional forward model for light propagation to a three-dimensional scattering problem. However, light escaped through the surface on the sides of the finger and did not contribute to the detector readings. Second, it is known that the distribution of the optical parameters is smoothed compared to the original parameter distribution (see Figures 8.4 and 8.5). Reconstructed heterogeneities with different optical parameters than the background medium do always appear larger than their actual size.